

Solar-Driven Carbon Dioxide Reduction: Can Photovoltaic-Biased Photoelectrocatalysis Beat Photovoltaic-Powered Electrocatalysis, and How?

Conglin Ye^{1,2}, Ying Zhang^{1,2}, Dong Liu^{1*}, Qiang Li^{1*}

1 School of Energy and Power Engineering, Nanjing University of Science and Technology, Nanjing 210094, China

2 These authors contributed equally

(*Corresponding Author)

ABSTRACT

The salient question addressed in this work is whether and how photovoltaic-biased photoelectrocatalysis (PV-PEC) can fairly and practically beat photovoltaic-powered electrocatalysis (PV-EC) for solar-driven carbon dioxide reduction (CO₂RR). First, it was argued that to fairly evaluate PV-PEC and PV-EC CO₂RR approaches in terms of techno-economy, the two devices should be driven by the same PV cell and produce the same group of products for the same series of Faradaic efficiency for each product. For this condition, PV-PEC CO₂RR was shown to surprisingly have higher solar-to-chemical conversion efficiency, and thereby more competitive, than PV-EC. This non-trivial performance was achieved by leveraging novel design of light management presented in this work and careful choice of PV and PEC cells achievable in literature. Furthermore, the framework generalized in this work is also applicable to other solar-driven catalytic processes with various different products such as productions of H₂O₂ by water oxidation and ammonia by nitrogen fixation.

Keywords: CO₂ reduction, photoelectrocatalysis, electrocatalysis, solar fuel, techno-economy

NONMENCLATURE

Abbreviations

PV	photovoltaic
PEC	photoelectrocatalysis
EC	electrocatalysis

STC	solar-to-chemical
CO ₂ RR	carbon dioxide reduction
<i>Symbols</i>	
η	energy conversion efficiency

1. INTRODUCTION

Converting carbon dioxide and water into useful chemicals using solar energy offers a means to provide an alternative to fossil fuels and to mitigate global warming. Since approximately 2.6 V voltage is needed for carbon dioxide reduction (CO₂RR), water oxidation and corresponding overpotentials [1], no single semiconductor can provide such a high voltage except for those having wide band gaps and thereby absorbing solar energy over a very narrow spectrum. Therefore, a photovoltaic (PV) cell that provides an extra bias, can be coupled to a photoelectrocatalysis (PEC) cell comprising a semiconductor photocathode for CO₂RR and a counter electrode for water oxidation. CO₂RR devices that employ the photovoltaic-biased photoelectrocatalysis (PV-PEC) approach [2], have shown higher solar-to-chemical (STC) energy conversion efficiency compared to those employ photocatalysis [3]. A PV cell can also power an electrocatalysis (EC) cell to construct a PV-EC CO₂RR device. For PV-PEC and PV-EC CO₂RR devices, the solar-to-chemical energy conversion efficiency, η_{STC} , is expressed as [1]

$$\eta_{\text{STC}} = \frac{J_{\text{op}} \times \sum_i (FE_i \times E_i^0)}{P_{\text{in}}} \quad (1)$$

where P_{in} is the incident solar power, FE_i and E_i^0 are the Faradaic efficiency and the thermodynamic potential of product i , and J_{op} is the operating current density of the device. The operating condition is determined as the cross point of the current density-voltage (J - V) curve of the PV cell and the J - V curve of the PEC or EC cells. Since the summation of the voltage produced by the photocathode and that by the PV cell, provides the necessary device voltage for PV-PEC, the PV cell in PV-PEC provides a smaller voltage than that in PV-EC, thereby generating a larger current density. Thus, a PV-PEC device has potentially higher η_{STC} than PV-EC according to Equation (1). However, the state-of-the-art STC efficiency for PV-PEC CO₂RR is 3.5% [2] which is much lower than the efficiency of 14.4% for PV-EC [4]. These efficiency numbers contradict what Equation (1) tells and skepticism has grown regarding PV-PEC as an alternative to PV-EC [5]. Therefore, the core question addressed in this work is whether PV-PEC CO₂RR can practically beat PV-EC, and how.

2. THEORY

Concept. We believe that the comparison of the efficiency numbers without any prerequisites is not fair to evaluate PV-PEC and PV-EC CO₂RR approaches; and thus, we proposed a new method to fairly compare their performance.

Let us revisit the STC efficiency of a PV-EC CO₂RR device. It can always operate at the maximum power point of the PV cell by using a power management unit (shown in Figure 1a) or by connecting more or fewer EC cells to the PV cell. Therefore, the STC efficiency of a PV-EC CO₂RR device, η_{PV-EC} , is expressed as

$$\eta_{PV-EC} = \eta_{PV} \times \frac{1}{V_{op}} \times \sum_i (FE_i \times E_i^0) \quad (2)$$

where η_{PV} is the solar-to-electricity conversion efficiency of the PV cell and V_{op} is the operating voltage of the EC cell. Equation (2) shows that, to fairly compare the performance of PV-EC and PV-PEC CO₂RR devices, they should be driven by the same PV cell (corresponding to the first term in Equation (2), η_{PV}); and the PV-EC CO₂RR device should operate at such V_{op} (corresponding to the second term, $1/V_{op}$) that PV-EC and PV-PEC CO₂RR devices produce the same group of products for the same series of Faradaic efficiency for each product (corresponding to the third term, $\sum(FE_i \times E_i^0)$).

Noteworthy, these prerequisites is self-consistent in terms of techno-economy. A comprehensive economic comparison of these two technologies, which are still under development, may be speculative and is beyond the scope of this work. However, it is interesting to

perform a thought experiment. Let us take the product price divided by the device cost as the measure [6]. CO₂RR products have various profitability [7], so the product prices of PV-PEC and PV-EC CO₂RR devices match if they produce the same group of products for the same series of Faradaic efficiency for each product. Their device costs, a large portion of which comes from the PV cell, are also comparable to each other if they are driven by the same PV cell. Therefore, for this condition, the approach with higher STC efficiency is more competitive.

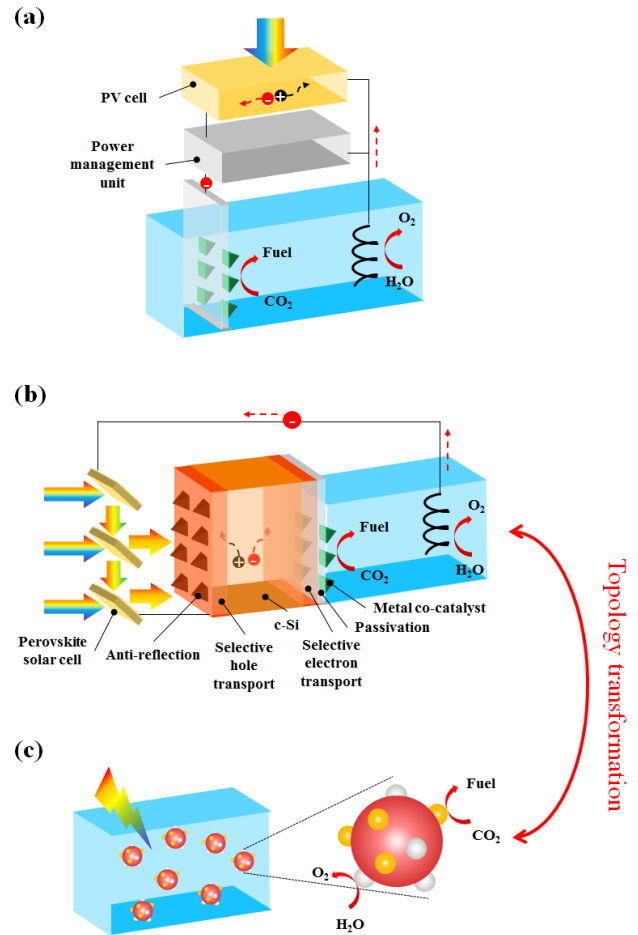


Figure 1. Solar-driven CO₂RR approaches investigated in this work. (a) PV-EC CO₂RR with a power management unit. (b) PV-PEC CO₂RR with the device architecture designed in this Viewpoint. (c) CO₂RR using suspended semiconductor nanoparticles with two different co-catalysts deposited on the surface, which is topologically transformed from PEC CO₂RR.

More insights can be given into Equation (2). First, it tells that η_{PV-EC} can be easily enhanced by using III-V multi-junction solar cells with high η_{PV} . However, the cost of this type of solar cells is very high; and thus, they are not practical for large scale applications. This also demonstrates that driven by the same PV cell is a necessary prerequisite to fairly compare PV-EC and PV-

PEC CO₂RR. Secondly, the same catalyst (usually metallic nanostructures) can be used for both the cathode in a PV-EC CO₂RR device, but also the co-catalyst of the photocathode in the counterpart PV-PEC CO₂RR device (shown in Figure 1b); and thus, PV-PEC and the counterpart PV-EC CO₂RR devices will produce the same group of products for the same series of Faradaic efficiency for each product, if they operate at the same current density (very often, the product selectivity of metallic catalysts varies drastically with the current density [8]). This is a specific feature of CO₂RR where high loading of metal co-catalyst nanoparticles or other nanostructures are required to increase selectivity to CO₂RR and to decrease H₂ production [9], and dominate the electrolysis properties of the photocathode as a result [2]. Therefore, our proposed comparison method is fair and viable.

3. RESULTS AND DISCUSSION

Proof-of-concept. In the first step, careful management of light and choice of PV and PEC cells were presented for PV-PEC CO₂RR to enhance its STC efficiency and resultantly improve its competitiveness.

In a PV-PEC device both PV and PEC cells absorb sunlight, from separated spectra though, and they overlap each other sharing the same area, unlike the configuration of a PV-EC device where only the PV cell absorbs light. In addition, although the overall voltage is the sum of the voltages of these two cells, the operating current density is limited by the smaller one determined by sunlight absorption of each cell. Therefore, the optical coupling between PV and PEC cells must be carefully optimized to enhance η_{STC} according to Equation (1). Toward this end, guided by careful light management, we proposed the PV-PEC CO₂RR device architecture shown in Figure 1b with following features. (1) Sunlight is illuminated from the un-reaction side of the photocathode. As mentioned above, high loading of metal co-catalyst is required to increase selectivity to CO₂RR. This co-catalyst layer has very low optical transmission [9-11] compared to the co-catalyst layer of photoelectrode for water splitting (for example higher than 90% in Abdi et al. [12]). Thus, sunlight absorption in the semiconductor absorber, the photocurrent density and the resultant η_{STC} according to Equation (1), would be reduced in a reaction-side-illumination architecture compared to the un-reaction-side-illumination one. (2) The PV cell is in front of the PEC cell so that the PV cell is not blocked by optically thick metal co-catalyst layer and thereby absorbs enough sunlight. (3) As a result, the semiconductor material in

the PEC cell has a narrower band gap than that in the PV cell so that the back PEC cell can absorb sunlight below the band gap wavelength of the semiconductor material in the front PV cell.

More insights can be given into the proposed architecture. The first is given to the semiconductor material used for the PEC cell. An anti-reflection layer is needed on the illumination side to maximize optical absorption. A selective hole transport layer on the illumination side, and a selective electron transport layer and a surface passivation layer on the reaction side, are also needed to promote carrier separation and transport. This analysis leads to our choice of crystalline silicon (c-Si), a mature narrow band gap semiconductor in industry, for scale-up, because commercial techniques can be used for c-Si processing including anti-reflection, passivation, and doping. The second is the solar cell. Since c-Si photocathode can provide a photo-voltage of about 0.6 V [2, 13], the solar cell must provide the rest 2.0 V to achieve target voltage of 2.6 V. This leads to our choice of two perovskite solar cells connected in series because they have suitable band gaps, high open circuit voltages and can be fabricated using potentially low cost methods [13]. Usually, semi-transparent perovskite solar cells should be used so that sunlight below their band gap wavelength can be transmitted to the c-Si photocathode. However, the efficiency of semi-transparent perovskite solar cells has been much lower compared to their opaque counterparts. Hence, we proposed the reflective-spectrum-splitting light management configuration so that high-efficiency opaque perovskite solar cells can be used for PV-PEC CO₂RR. As shown in Figure 1b, this configuration, inspired by window blinds [14-16], features an array of solar cell panels comprising one side coated by perovskite solar cell and another specular reflective side, or with perovskite solar cells on both sides, so sunlight below their band gap wavelength is not transmitted, but reflected to the c-Si photocathode; and thus, state-of-the-art opaque planar perovskite solar cells can be used. So far, it is noteworthy that the proposed PV-PEC CO₂RR device (Figure 1b) is totally different from diverse devices reported in literature [2, 9-12, 17-20].

Now, let us compare the performance of PV-PEC CO₂RR and its counterpart PV-EC CO₂RR. η_{STC} is determined by Equation (1) where the current density-voltage (J-V) curves of both PV and PEC/EC cells are needed. The J-V curve of the PV cell can be approximated by the ideal diode equation [20] expressed as

$$J = J_{sc} - J_0 \left[\exp\left(\frac{qV}{kT}\right) - 1 \right] \quad (3)$$

where experimental short-circuit current density ($J_{sc} = 19.00 \text{ mA cm}^{-2}$) and open-circuit voltage ($V_{oc} = 1.19 \text{ V}$) reported in a recent work by our group [16] for a single perovskite solar cell (1.66 eV band gap) are the input parameters. For two perovskite solar cells connected in series, J_{sc} will be reduced by a factor of two with V_{oc} being doubled. The black dashed curve in Figure 2a shows the J - V curve of two of these perovskite solar cells connected in series. This perovskite solar cell was chosen for three reasons. (1) It employs planar structure which is a requisite for the reflective spectrum splitting configuration. (2) Two of these perovskite solar cells connected in series can produce high V_{oc} of 2.38 V. (3) They can also produce J_{sc} of 9.50 mA cm^{-2} rendering η_{STC} higher than 10% corresponding to Equation (1). This J_{sc} is also lower than the mass-transfer-limited current density for a device with CO_2 dissolved in the aqueous electrolyte. [2]

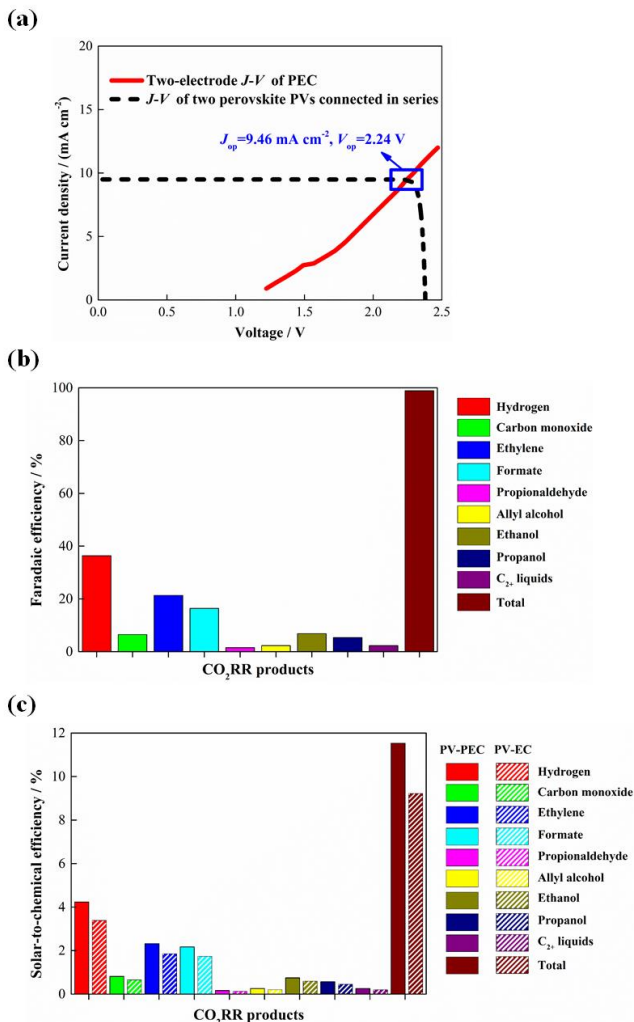


Figure 2. Performance of PV-PEC CO_2RR and the counterpart PV-EC CO_2RR . (a) J - V curve of two perovskite solar cells

connected in series and two-electrode J - V curve of PEC cell with the photocathode comprising a c-Si photoabsorber and a high loading of nanostructured Cu-Ag bimetallic co-catalyst. (b) Faradaic efficiency of each product for both PV-PEC CO_2RR and the counterpart PV-EC at 9.46 mA cm^{-2} . (c) Achievable STC efficiency of PV-PEC CO_2RR and the counterpart PV-EC for each product and all products.

The two-electrode J - V curve of the PEC cell with the photocathode comprising a c-Si photoabsorber and a high loading of metal co-catalyst, can be calculated from the measured J - V behavior of a c-Si photoabsorber for light condition and the measured two-electrode J - V curve of an electrocatalysis cell using a metallic cathode for dark condition [21,22], because the electrolysis properties of the photocathode were dominated by the metal co-catalyst, and the light harvesting process of the c-Si photoabsorber and the electrolysis process of the metal co-catalyst are resultantly decoupled from each other. As mentioned above, the same metal catalyst is used for both the photocathode in PV-PEC CO_2RR but also the cathode in the counterpart PV-EC CO_2RR , so we took the results for the nanostructured Cu-Ag bimetallic catalyst reported in Gurudayal et al. [23] as an example. The cathode employing this catalyst showed high selectivity to the production of hydrocarbons and oxygenates that can exploit existing infrastructures. Moreover, its required voltage at the current density of $\sim 10 \text{ mA cm}^{-2}$ can be provided by the summation of the photo-voltages generated from the PV cell and the c-Si photoabsorber. The J - V behavior of the c-Si photoabsorber for light condition was also approximated by the ideal diode equation. In the proposed architecture (Figure 1b), the PV cell is in front of the PEC cell, so the back c-Si photoabsorber receives less sunlight and thus, generates smaller J_{sc} . The perovskite solar cell absorbs sunlight below 747 nm (1.66 eV), thereby reducing the J_{sc} of the c-Si photoabsorber by 55%. Therefore, the input parameters into the diode equation are experimental short-circuit current density (30 mA cm^{-2}) reduced by 55% and open-circuit voltage (0.6 V) reported for the c-Si photoabsorber [2]. Then, the two-electrode J - V curve of the PEC cell with the photocathode comprising a c-Si photoabsorber and a high loading of nanostructured Cu-Ag bimetallic co-catalyst was calculated and shown as the red curve in Figure 2a.

This model device of PV-PEC CO_2RR operates at 9.46 mA cm^{-2} and 2.24 V as shown in Figure 2a with the corresponding Faradaic efficiency of each product shown in Figure 2b. This operating condition is very close to the maximum power point of the PV cell as a result of novel light management and careful cell

choice. The solar-to-chemical conversion efficiency for each product was shown in Figure 2c with their thermodynamic potential listed in Table 1. The solar-to-chemical conversion efficiency, η_{PV-PEC} , for all products is as high as 11.5% with a notable efficiency of 6.5% for producing hydrocarbons and oxygenates. It must be emphasized that these efficiency numbers are achievable right away. Then, the V_{op} of the counterpart PV-EC CO₂RR device was obtained from the J - V behavior reported in Gurudayal et al. [23] to be 2.81 V corresponding to the current density of 9.46 mA cm⁻². The solar-to-chemical conversion efficiency of this counterpart device, which is driven by the same two perovskite solar cells connected in series, was also shown in Figure 2c. Noteworthy, η_{PV-EC} for all products is 9.2%, which is beaten by η_{PV-PEC} of 11.5%. These results demonstrate the superiority of PV-PEC CO₂RR over PV-EC CO₂RR. Again, this non-trivial performance, which has never been demonstrated before, is attributed to our novel design of light management and careful choice of both the PV and PEC cells.

Table 1. CO₂RR products and their thermodynamic potentials.

Product		Thermodynamic potential (V)
Total	Hydrogen	1.23
	Carbon monoxide	1.33
Hydrocarbons and oxygenates	Ethylene	1.15
	Formate	1.40
	Propionaldehyde	1.14
	Allyl alcohol	1.18
	Ethanol	1.15
	Propanol	1.13
	Other C ₂₊ liquids	~1.20

4. CONCLUSIONS

In this work, the advantage of PV-PEC over PV-EC has been demonstrated for solar-driven CO₂RR in terms of techno-economy. We must further emphasize that the framework generalized in this work is also applicable to other solar-driven catalytic processes with various different products such as productions of H₂O₂ by water oxidation and ammonia by nitrogen fixation [24,25]. Moreover, PEC can be topologically transformed to the approach of suspended semiconductor nanoparticles with two different co-catalysts deposited on the surface (shown in Figure 1c) [26,27], rendering it a much cheaper technology. Therefore, this work, in combination with a previous

viewpoint demonstrating the advantage of PEC in terms of selectivity [8], motivates PEC investigations for high-performance solar-driven catalytic technologies.

ACKNOWLEDGEMENT

This work was supported by the Basic Science Center Program for Ordered Energy Conversion of the National Natural Science Foundation of China (No.51888103).

REFERENCE

- [1] White JL, Baruch MF, Pander JE, Hu Y, Fortmeyer IC, Park JE, Zhang T, Liao K, Gu J, Yan Y, Shaw TW, Abelev E, Bocarsly AB. Light-Driven Heterogeneous Reduction of Carbon Dioxide: Photocatalysts and Photoelectrodes. *Chemical Reviews* 2015;115:12888-935.
- [2] Grudayal, Beeman JW, Bullock J, Wang H, Eichhorn J, Towle C, Javey A, Toma FM, Mathews N, Ager JW. Si photocathode with Ag-supported dendritic Cu catalyst for CO₂ reduction. *Energy & Environmental Science* 2019;12: 1068-77.
- [3] Sorcar S, Hwang Y, Lee J, Kim H, Grimes KM, Grimes CA, Jung JW, Cho CH, Majima T, Hoffmann MR, In SI. CO₂, water, and sunlight to hydrocarbon fuels: a sustained sunlight to fuel (Joule-to-Joule) photo-conversion efficiency of 1%. *Energy & Environmental Science* 2019;12:2685-96.
- [4] Schreier M, Heroguel F, Steier L, Ahmad S, Luterbacher JS, Mayer MT, Luo J, Gratzel M. Solar conversion of CO₂ to CO using Earth-abundant electrocatalysts prepared by atomic layer modification of CuO. *Nature Energy* 2017;2:17087.
- [5] Jacobsson TJ. Photoelectrochemical water splitting: an idea heading towards obsolescence? *Energy & Environmental Science* 2018;11:1977-9.
- [6] Jacobsson TJ, Fjallstrom V, Edoff M, Edvinsson T. Sustainable solar hydrogen production: from photoelectrochemical cells to PV-electrolyzers and back again. *Energy & Environmental Science* 2014;7:2056-70.
- [7] Singh MR, Clark EL, Bell AT. Thermodynamic and achievable efficiencies for solar-driven electrochemical reduction of carbon dioxide to transportation fuels. *Proc Natl Acad Sci USA* 2015;112:E6111-E8.
- [8] Beranek R. Selectivity of Chemical Conversions: Do Light-Driven Photoelectrocatalytic Processes Hold Special Promise? *Angew Chem-Int Edit* 2019;58:2-8.
- [9] Song JT, Ryoo H, Cho M, Kim J, Kim JG, Chung SY, Oh J. Nanoporous Au Thin Films on Si Photoelectrodes for Selective and Efficient Photoelectrochemical CO₂ Reduction. *Advanced Energy Materials* 2017;7:1601103.

- [10] Jang YJ, Jeong I, Lee J, Lee J, Ko MJ, Lee JS. Unbiased Sunlight-Driven Artificial Photosynthesis of Carbon Monoxide from CO₂ Using a ZnTe-Based Photocathode and a Perovskite Solar Cell in Tandem. *Acs Nano* 2016;10: 6980-6987-3604.
- [11] Hu YP, Chen FJ, Ding P, Yang H, Chen JM, Zha CY, Li YG. Designing effective Si/Ag interface via controlled chemical etching for photoelectrochemical CO₂ reduction. *Journal of Materials Chemistry A* 2018;6:21906.
- [12] Abdi FF, Han LH, Smets AHM, Zeman M, Dam B, van de Krol R. Efficient solar water splitting by enhanced charge separation in a bismuth vanadate-silicon tandem photoelectrode. *Nature Communications* 2013;4: 2195.
- [13] Green MA, Dunlop ED, Levi DH, Hohl-Ebinger J, Yoshita M, Ho-Baillie AWY. Solar cell efficiency tables (version 54). *Prog Photovoltaics* 2019;27:565-75.
- [14] Liu D, Yu HT, Duan YY, Li Q, Xuan YM. New Insight into the Angle Insensitivity of Ultrathin Planar Optical Absorbers for Broadband Solar Energy Harvesting. *Scientific Reports* 2016;6: 32515.
- [15] Liu D, Li Q. Sub-nanometer planar solar absorber. *Nano Energy* 2017;34:172-80.
- [16] Zheng LK, Wang JL, Xuan YM, Yan MY, Yu XX, Peng Y, Cheng YB. A perovskite/silicon hybrid system with a solar-to-electric power conversion efficiency of 25.5%. *Journal of Materials Chemistry A* 2019;7:26479-89.
- [17] Li CC, Wang T, Liu B, Chen MX, Li A, Zhang G, Du M, Wang H, Liu SF, Gong J. Photoelectrochemical CO₂ reduction to adjustable syngas on grain-boundary-mediated a-Si/TiO₂/Au photocathodes with low onset potentials. *Energy & Environmental Science* 2019;12:923-8.
- [18] Jang YJ, Jang JW, Lee J, Kim JH, Kumagai H, Lee J, Minegishi T, Kubota J, Domen K, Lee SJ. Selective CO production by Au coupled ZnTe/ZnO in the photoelectrochemical CO₂ reduction system. *Energy & Environmental Science* 2015;8:3597-604.
- [19] Young JL, Steiner MA, Doscher H, France RM, Turner JA, Deutsch TG. Direct solar-to-hydrogen conversion via inverted metamorphic multi-junction semiconductor architectures. *Nature Energy* 2017;2: 17028.
- [20] Dotan H. Beating the Efficiency of Photovoltaics-Powered Electrolysis with Tandem Cell Photoelectrolysis. *Acs Energy Letters* 2017;2:45-51.
- [21] Coridan RH, Nielander AC, Francis SA, McDowell MT, Dix V, Chatman SM, Lewis NS. Methods for comparing the performance of energy-conversion systems for use in solar fuels and solar electricity generation. *Energy & Environmental Science* 2015;8:2886-901.
- [22] Zhou XH, Liu R, Sun K, Chen YK, Verlage E, Francis SA, Lewis NS, Xiang C. Solar-Driven Reduction of 1 atm of CO₂ to Formate at 10% Energy-Conversion Efficiency by Use of a TiO₂-Protected III-V Tandem Photoanode in Conjunction with a Bipolar Membrane and a Pd/C Cathode. *Acs Energy Letters* 2016;1:764-70.
- [23] Gurudayal, Bullock J, Sranko DF, Towle CM, Lum YW, Hettick M, Scott MC, Javey A, Ager JW. Efficient solar-driven electrochemical CO₂ reduction to hydrocarbons and oxygenates. *Energy & Environmental Science* 2017;10:2222-30.
- [24] Liu JL, Zou YS, Jin BJ, Kan Z, Park JH. Hydrogen Peroxide Production from Solar Water Oxidation. *Acs Energy Letters* 2019;4:3018-27.
- [25] Xue F, Si YT, Wang M, Liu MC, Guo LJ. Toward efficient photocatalytic pure water splitting for simultaneous H₂ and H₂O₂ production. *Nano Energy* 2019;62:823-31.
- [26] Ardo S, Rivas DF, Modestino MA, Greiving VS, Abdi FF, Alarcon Llado E, et al. Pathways to electrochemical solar-hydrogen technologies. *Energy & Environmental Science* 2018;11:2768-83.
- [27] Tilley SD. Recent Advances and Emerging Trends in Photo-Electrochemical Solar Energy Conversion. *Advanced Energy Materials* 2019;9: 1802877.